

## Lock-exchange problem for Boussinesq fluids revisited: Exact shallow-water solution

Gerasimos Politis<sup>1</sup> and Jānis Priede<sup>1, a)</sup>

*Fluid and Complex Systems Research Centre, Coventry University, Coventry,  
CV1 5FB, United Kingdom<sup>b)</sup>*

An exact solution to the lock-exchange problem, which is a two-layer analogue of the classical dam-break problem, is obtained in the shallow-water (SW) approximation for two immiscible fluids with slightly different densities. The problem is solved by the method of characteristics using analytic expressions for the Riemann invariants. The obtained solution, which represents an inviscid approximation to the high-Reynolds-number limit, is in general discontinuous containing up to three hydraulic jumps which are due to either multivaluedness or instability of the continuous SW solution. Hydraulic jumps are resolved by applying the Rankine-Hugoniot conditions for the SW mass and generalized momentum conservation equations. The latter contains a free parameter  $\alpha$  which defines the relative contribution of each layer to the interfacial pressure gradient. We consider a solution for  $\alpha = 0$ , which corresponds to both layers affecting the interfacial pressure gradient with equal weight coefficients. This solution is compared with the solutions resulting from the application of the classical Benjamin's front condition as well as the circulation conservation condition, which correspond to  $\alpha = -1$  and  $\alpha \rightarrow \infty$ , respectively. The SW solution reproduces all principal features of 2D numerical solution for viscous fluids. The gravity current speed is found to agree well with experimental and numerical results when the front acquires the largest stable height which occurs at  $\alpha = \sqrt{5} - 2$ . We show that two-layer SW equations for the mass and generalized momentum conservation can describe interfacial waves containing hydraulic jumps in a self-contained way without external closure conditions.

---

<sup>a)</sup>Also at Department of Physics, University of Latvia, Riga, LV-1004, Latvia

<sup>b)</sup>Electronic mail: j.priede@coventry.ac.uk

## I. INTRODUCTION

Although inertia-dominated fluid flows tend to be very complex, especially in the presence of a free surface or interface, there are certain hydrodynamic problems of this type which can be solved analytically. A well-known example is the classic dam-break problem in which an instantaneous collapse of the reservoir wall causes a mass of water to be driven by gravity over a horizontal or sloped ground.<sup>1,2</sup> This problem was originally solved by Barré de Saint-Venant<sup>3</sup> and then shortly afterwards in a more complete form by Ritter<sup>4</sup> using the shallow-water (SW) approximation and the method of characteristics.

There is an analogous problem for a stably-stratified two-layer system, which is known as the lock-exchange problem, where a heavier fluid in a horizontal channel is initially separated by a vertical lock from a lighter fluid on the other side. When the lock gate is rapidly removed, the difference in hydrostatic pressure causes the heavier fluid to intrude along the bottom into the lighter fluid which in turn is forced to flow back at the top. Such flows produced by the lock exchange, which are commonly referred to as gravity currents, have extensively been studied experimentally due to their occurrence in various natural and artificial environments.<sup>5-7</sup>

If the heavier fluid is covered by a much lighter ambient fluid, the lock-exchange problem reduces to that of the dam-break. Likewise, the two-layer problem reduces to that of the single-layer when the bottom layer is much thinner than the upper layer which, in this case, just modifies the effective value of gravity.<sup>1</sup> Although the two-layer problem becomes mathematically equivalent to that of the single-layer in this limit, the actual flows have substantial differences. Namely, the heavy fluid is observed to form a bore, i.e., a finite-height front, as it propagates along the bottom into the lighter fluid whereas the ideal dam-break solution predicts a sharp front edge.<sup>8</sup> This has led to a common assumption that the SW equations for two-layer system are inherently incomplete and unable to describe internal bores without external closure relations.<sup>9</sup> The latter have to be deduced by dimensional arguments<sup>8</sup> or derived using various semi-empirical and approximate integral models.<sup>10</sup>

For fluids with nearly equal densities, which can be described using the Boussinesq approximation,<sup>11</sup> the SW equations for two-layer system bounded by a rigid lid become identical with the single-layer equations when both are cast in canonical form using the Riemann

invariants.<sup>12</sup> This fact was used by Chumakova *et al.*<sup>13</sup> to suggest that the lock-exchange problem for Boussinesq fluids is mathematically equivalent to the single-layer dam-break problem. Esler and Pearce<sup>14</sup> argue that this equivalence is limited by different physical variables of the two-layer problem mapping to the same Riemann invariants. This makes the inverse mapping non-unique and results in the lock-exchange flows which have no dam-break counterparts. However, it has not been realized so far that the lock-exchange problem for Boussinesq fluids is solvable analytically using the hydrostatic SW approximation and the method of characteristics like the dam-break problem. The present paper aims to fill this gap by providing a comprehensive analytical solution of this generic hydrodynamic problem.

Various hydraulic-type models<sup>15–17</sup> and approximate *ad hoc* solutions<sup>18,19</sup> have been proposed for the lock-exchange problem. One of the most notable is the model of Shin, Dalziel, and Linden<sup>7</sup> where the flow is assumed to consist of a gravity current which is connected to the lock by a bore propagating upstream. A good agreement with experimentally observed height of gravity current is achieved when the momentum and energy are assumed to be conserved by the system of two jumps rather than by each jump separately. Borden and Meiburg<sup>20</sup> find that this model fares much worse when the conservation of circulation is imposed instead of that of momentum. They attribute this shortcoming of the model to its over-simplicity. It is also not clear what physical mechanism could account for the energy generated by the bore. In the SW framework, energy generating bores are unphysical.

Klemp, Rotunno, and Skamarock<sup>6</sup> solve the lock-exchange problem numerically by using a characteristics-type method suggested by Rottman and Simpson<sup>17</sup>. This approach, however, differs significantly from the standard simple-wave method<sup>21</sup> (Sec. 6.8) pursued in this study. Hogg<sup>22</sup> uses a hodograph transform to solve the problem analytically in the reduced gravity approximation. Effectively, this is a single-layer solution, which is limited to large density differences. A direct numerical solution of the problem has been attempted by Ungarish (Sec. 2.4)<sup>23</sup> using non-conservative two-layer SW equations. The discontinuous solutions obtained in such a way are inherently spurious because they do not satisfy relevant conservation laws. A lock-exchange problem with entrainment has been modeled numerically by Milewski and Tabak<sup>24</sup> using the two-layer SW conservation laws for the circulation and energy and an advanced finite-volume scheme. They also use a characteristics-type method similar to that of Rottman and Simpson<sup>17</sup> to obtain an analytical solution to the problem

with the conservation of either the mass or energy besides that of circulation. Partial lock-exchange problem for Boussinesq fluids has been solved numerically by Esler and Pearce<sup>14</sup> using a weakly non-hydrostatic SW approximation in which the wave dispersion prevents the formation of sharp fronts. Recently, this problem was revisited by Khodkar, Nasr-Azadani, and Meiburg<sup>25</sup> using the so-called differential vorticity model. Although the authors presume their model to be non-hydrostatic, it produces the same characteristic equation as the hydrostatic two-layer SW approximation.<sup>6,17</sup> It implies that this model is mathematically equivalent to the SW circulation conservation law which, in turn, corresponds the singular limit  $\alpha \rightarrow \infty$  of the generalized SW momentum equation considered in the present study.

The paper is organized as follows. In the next section, we formulate the problem and introduce a mathematical model based on the generalized SW momentum equation. In section III, we use the method of characteristics for simple waves to solve the problem analytically. An alternative version of the lock exchange problem with a modified initial state and the corresponding analytical solution are presented in section IV. In section V, the original lock exchange problem is solved numerically using a composite Lax-Wendroff/Lax-Friedrichs scheme to integrate locally conservative two-layer SW equations. The paper is concluded with a summary and discussion of the main results in section VI.

## II. FORMULATION OF PROBLEM

Consider a horizontal channel of constant height  $H$  bounded by two parallel solid walls and filled with two inviscid immiscible fluids which are subject to a downward gravity force with the free fall acceleration  $g$ . Initially, a layer of heavier fluid of density  $\rho^+$  and uniform depth  $h^+$  is overlaid by a lighter fluid of density  $\rho^-$  and separated by a vertical lock gate from the same lighter fluid on the right as shown in Fig. 1. The lock is instantaneously released and the heavier fluid starts to penetrate along the bottom into the lighter fluid so forcing the latter in the opposite direction at the top.

In the first-order (hydrostatic) SW approximation, which is based on the assumption that the characteristic horizontal length scale  $L$  is much larger than the height  $H$  :  $H/L = \varepsilon \ll 1$ , the mass conservation results in the vertical velocity component  $w$  which is much smaller than the characteristic horizontal velocity  $u$  :  $w/u \sim \varepsilon$ . Such an effectively horizontal flow

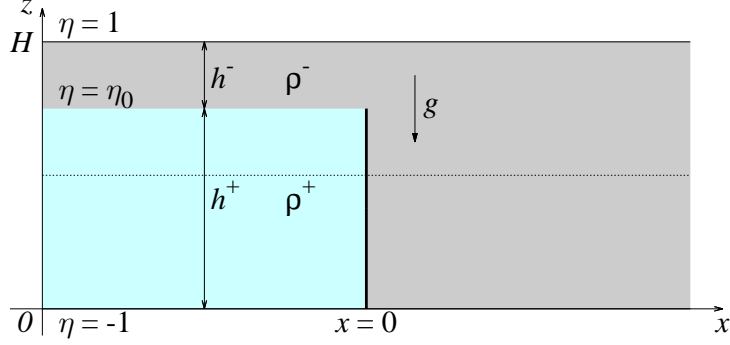


Figure 1. Sketch of the initial state of the lock-exchange problem.

has a dynamically negligible effect on the vertical pressure distribution which is thus purely hydrostatic:

$$p^\pm(x, z, t) = \Pi(x, t) - \rho^\pm g(z - h(x, t)). \quad (1)$$

The plus and minus indices refer to the bottom and top layers, respectively, and  $\Pi(x, t) = p^\pm(x, z, t)|_{z=h}$  is the pressure distribution along the interface. Substituting the pressure distribution (1) into the Euler equation for the horizontal velocity component  $u^\pm$  in each layer yields the first SW equation, while the second equation follows from the conservation of mass in each layer:<sup>26</sup>

$$\rho(u_t + uu_x \pm gh_x) = -\Pi_x, \quad (2)$$

$$h_t + (uh)_x = 0. \quad (3)$$

The subscripts  $t$  and  $x$  stand for the corresponding partial derivatives and the plus and minus indices at  $\rho$ ,  $u$ , and  $h$  have been dropped for the sake of brevity. Note that in the SW approximation, which is a long-wave approximation, the relevant flow features with the characteristic length scale comparable to the layer depth appear as hydraulic jumps.

The system of four SW equations (2,3) contains five unknowns,  $u^\pm$ ,  $h^\pm$  and  $\Pi$ , and is completed by adding the fixed height constraint  $\{h\} \equiv h^+ + h^- = H$ , which can be used to eliminate the top layer depth  $h^- = H - h^+$ . Henceforth, the curly brackets denote the sum of the enclosed quantities.

Two more unknowns can be eliminated as follows. First, adding up the mass conservation equations for both layers and using  $\{h\}_t \equiv 0$ , we obtain  $\{uh\} = \Phi(t)$ , which is the total flow rate. The channel is assumed to be laterally closed. It corresponds to  $\Phi \equiv 0$ , and thus

$u^- h^- = -u^+ h^+$ . Second, the pressure gradient  $II_x$  can be eliminated by subtracting Eq. (2) for the top layer from that for the bottom layer. This leaves only two unknowns,  $U \equiv u^+ h^+$  and  $h = h^+$ , and two equations, which can be written in locally conservative form as follows

$$(\{\rho/h\} U)_t + \left(\frac{1}{2} [\rho/h^2] U^2 + g[\rho]h\right)_x = 0, \quad (4)$$

$$h_t + U_x = 0. \quad (5)$$

The square brackets above denote the difference of the enclosed quantities between the bottom and top layers:  $[f] \equiv f^+ - f^-$ .

In the following, the density difference is assumed to be small. According to the Boussinesq approximation, this difference is important only for the gravity of fluids, which drives the flow, but not for the inertia of fluids. The problem is simplified further by using the total height  $H$  and the characteristic gravity wave speed  $C = \sqrt{2Hg[\rho]/\{\rho\}}$  as the length and velocity scales, and  $H/C$  as the time scale.

Then Eqs. (4,5) take a remarkably symmetric form:<sup>24</sup>

$$\vartheta_t + \frac{1}{2}(\eta(1 - \vartheta^2))_x = 0, \quad (6)$$

$$\eta_t + \frac{1}{2}(\vartheta(1 - \eta^2))_x = 0, \quad (7)$$

where  $\eta = [h]$  and  $\vartheta = [u]$  are the dimensionless depth and velocity differentials between the top and bottom layers. Subsequently, the former is referred to as the interface height and the latter as the shear velocity. The momentum and energy equations

$$(\eta\vartheta)_t + \frac{1}{4}(\eta^2 + \vartheta^2 - 3\eta^2\vartheta^2)_x = 0, \quad (8)$$

$$(\eta^2 + \vartheta^2 - \eta^2\vartheta^2)_t + (\eta\vartheta(1 - \eta^2)(1 - \vartheta^2))_x = 0, \quad (9)$$

can be obtained by multiplying Eq. (6) with  $\eta$  and  $\eta^2\vartheta$ , respectively, and then using Eq. (7) to convert the resulting equations into locally conservative form. Note that the conserved quantity  $\eta\vartheta$  in Eq. (8) represents a pseudo-momentum (impulse).<sup>27</sup> An infinite sequence of further conservation laws can be constructed in a similar way.<sup>24</sup> The generalized momentum equation can be obtained by multiplying Eq. (6) with an arbitrary constant  $\alpha$  and adding to Eq. (8):

$$((\eta + \alpha)\vartheta)_t + \frac{1}{4}(\eta^2 + \vartheta^2 - 3\eta^2\vartheta^2 + 2\alpha\eta(1 - \vartheta^2))_x = 0. \quad (10)$$

For more detailed derivation of Eqs. (8)–(10), we refer to Priede<sup>27</sup>. The constant  $\alpha$  in Eq. (10), which defines the relative contribution of each layer to the pressure gradient along the interface, is supposed to depend only on the ratio of densities. For nearly equal densities,  $\alpha \approx 0$  is expected, which corresponds to both layers affecting the pressure at the interface with equal weight coefficients. In the following, we will obtain an analytical solution for general  $\alpha$  and then focus on three particular cases:  $\alpha = 0, \infty, -1$ . The first two correspond to the momentum and circulation conservation laws (8) and (6), whereas the third one reproduces the classical front condition for gravity currents obtained by Benjamin<sup>15</sup> as well as its generalization to internal bores by Klemp, Rotunno, and Skamarock<sup>28</sup>. The alternative front condition for internal bores proposed by Wood and Simpson<sup>29</sup> is reproduced by  $\alpha = 1$  but not considered here because it is not applicable to gravity currents which are the key element of the lock-exchange flow.

Equations (6) and (7) can be written in canonical form as follows

$$R_t^\pm + \lambda^\pm R_x^\pm = 0 \quad (11)$$

using the characteristic velocities

$$\lambda^\pm = \frac{3}{4}R^\pm + \frac{1}{4}R^\mp \quad (12)$$

and the Riemann invariants<sup>10,12,14,30–32</sup>

$$R^\pm = -\eta\vartheta \pm \sqrt{(1-\eta^2)(1-\vartheta^2)}, \quad (13)$$

which are the constants of integration of the characteristic form of Eqs. (6) and (7):

$$\frac{d\vartheta}{d\eta} = \mp \sqrt{\frac{1-\vartheta^2}{1-\eta^2}}. \quad (14)$$

Note that along two trajectories  $x^\pm(t)$  defined in the  $(x, t)$  plane by  $\frac{dx^\pm}{dt} = \lambda^\pm$ , Eq. (11) with the respective index reduces to  $\frac{dR^\pm}{dt} = 0$ . It means that the respective Riemann invariant is constant along that trajectory which is referred to as the characteristic curve.<sup>21</sup> This is the basic idea behind the method of characteristics which we use to solve the problem analytically.

Since the interface is confined between the top and bottom boundaries, which corresponds to  $\eta^2 \leq 1$ , the characteristic velocities (12) are real and, thus, the equations are of hyperbolic

type if  $\vartheta^2 \leq 1$ . The latter constraint on the shear velocity is required for the stability of interface which would be otherwise disrupted by a long-wave Kelvin-Helmholtz instability.<sup>33</sup> It has to be noted that this instability is different to the usual short-wave Kelvin-Helmholtz which is absent in the hydrostatic SW approximation.<sup>14</sup>

Integrating Eqs. (7) and (10) across a discontinuity at the point  $x = \xi(t)$ , where  $\eta$  and  $\vartheta$  have the jumps  $[[\eta]] \equiv \eta_+ - \eta_-$  and  $[[\vartheta]] \equiv \vartheta_+ - \vartheta_-$  with the plus and minus subscripts denoting the corresponding quantities in the front and back of the jump, and the double-square brackets stand for the differentials of the enclosed quantities across the jump, the jump propagation velocity can be expressed respectively as follows<sup>27</sup>

$$\dot{\xi} = \frac{1}{2} \frac{[[\vartheta(1 - \eta^2)]]}{[[\eta]]}, \quad (15)$$

$$\dot{\xi} = \frac{1}{4} \frac{[[\vartheta^2(1 - 2\eta^2) + \eta(\eta + 2\alpha)(1 - \vartheta^2)]]}{[[\eta + \alpha)\vartheta]]}. \quad (16)$$

As for single layer, the jump conditions above consist of two equations and contain five unknowns,  $\eta_{\pm}$ ,  $\vartheta_{\pm}$  and  $\dot{\xi}$ . It means that two unknown parameters can be determined when the other three are known.

As the jump conditions (15,16) are non-linear, multiple solutions are in principle possible. Some of these solutions may be unphysical. For a solution to be feasible, it has to satisfy the hyperbolicity constraint  $\vartheta_{\pm}^2 \leq 1$  as well as the energy constraint which follows from the integration of Eq. (9) across the jump and defines the associated energy production rate:<sup>27</sup>

$$[[\eta\vartheta(1 - \eta^2)(1 - \vartheta^2)]] - \dot{\xi} [[\eta^2 + \vartheta^2 - \eta^2\vartheta^2]] = \dot{\epsilon} \leq 0. \quad (17)$$

This quantity cannot be positive as the energy can only be dissipated but not generated in the jump.

### III. ANALYTICAL SIMPLE-WAVE SOLUTION

In this section, the lock-exchange problem will be solved analytically using the simple-wave method<sup>21</sup> along with the analytic expressions for the Riemann invariants (13) and the associated characteristic velocities (12). To facilitate the solution it is useful to introduce the following substitutions:

$$\eta = \sin \theta, \quad (18)$$

$$\vartheta = \sin \phi, \quad (19)$$



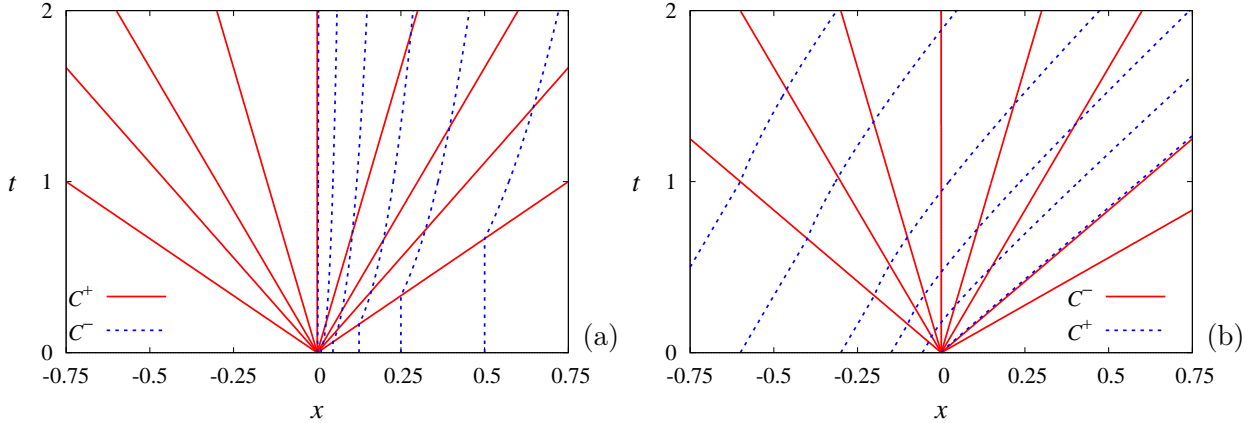


Figure 2. The  $C^+$  and  $C^-$  characteristics in the downstream ( $x > 0$ ) (a) and upstream ( $x < 0$ ) (b) regions for the partial lock exchange with  $\eta_0 = \cos \theta_0$ .

where  $\theta$  and  $\phi$  are the associated angular variables. In these variables, the Riemann invariants and the characteristic velocities can be written more concisely as follows

$$r^\pm = \pm \arccos R^\pm = \phi \pm \theta, \quad (20)$$

$$\lambda^\pm = \pm \frac{3}{4} \cos r^\pm \mp \frac{1}{4} \cos r^\mp. \quad (21)$$

The simple-wave method is applicable to the disturbances which propagate into an initially homogeneous state. In this problem, there are two such states: one on the right from the lock ( $x > 0$ ) with the interface located at the bottom ( $\eta = -1$ ) and the second on the left ( $x < 0$ ) with the interface located at  $\eta = \eta_0$ . Subsequently, these regions will be referred to as the downstream and upstream states according to the direction in which the heavier fluid flows.

Let us start with the downstream region, which is completely filled with the lighter fluid, and consider the disturbances propagating from the lock along the  $C^+$  characteristics into this uniform state where  $(\eta, \vartheta) = (-1, 0)$  and, correspondingly,  $(\theta, \phi) = (-\frac{\pi}{2}, 0)$ . Then the respective Riemann invariant along the  $C^-$  characteristics, which originate from this state, is  $r^- = \phi - \theta = \frac{\pi}{2}$ . Applying this result to the  $C^+$  characteristics, which propagate from the lock into this state, this Riemann invariant can be written as follows

$$r^+ = \phi + \theta = \frac{\pi}{2} + 2\theta,$$

and hence

$$\lambda^+(\theta) = -\frac{3}{4} \sin 2\theta = \frac{dx}{dt}. \quad (22)$$

Since not only  $r^+$  but also  $r^-$  are invariant along  $C^+$ , owing to Eq. (21) the same holds also for  $\lambda^+$ . Then Eq. (22) can be integrated to obtain  $\lambda^+ = \frac{x}{t}$ , which defines  $C^+$  characteristics as the straight lines emanating from the origin of the  $(x, t)$  plane. This straightforwardly leads to the solution, which can be written in parametric form as follows

$$\frac{x}{t} = -\frac{3}{4} \sin 2\theta, \quad (23)$$

$$\eta^+ = \sin \theta, \quad (24)$$

$$\vartheta^+ = \cos \theta. \quad (25)$$

The  $C^-$  slope, which is given by the corresponding characteristic velocity and can be expressed as

$$\lambda^- = -\frac{1}{4} \sin 2\theta = \frac{1}{3} \lambda^+, \quad (26)$$

varies along the  $C^-$  characteristics as they cross the  $C^+$  characteristics. At  $\theta = 0$ , the slopes of both families of characteristics become equal to each other:  $\lambda^+ = \lambda^- = 0$ . It means that the region where both families of characteristics intersect, and thus solutions (24) and (25) are applicable, is limited to  $-\frac{\pi}{2} \leq \theta \leq 0$ . Equation (26) written in terms of  $x$  and  $t$  takes the form

$$\frac{dx}{dt} = \frac{1}{3} \frac{x}{t}$$

and defines the  $C^-$  characteristics above the rightmost  $C^+$  characteristic, *i.e.*, for  $x \geq \frac{3}{4}t$ . The general solution of this equation is  $x(t) = ct^{1/3}$ , where the unknown constant  $c$  can be determined by matching this solution with  $x(t) = \text{const}$  for  $0 \leq x \leq \frac{3}{4}t$ , which corresponds to  $\lambda^\pm = 0$  for the undisturbed downstream state. Both families of characteristics for the downstream region are shown in Fig. 2(a).

For the full lock exchange ( $\eta_0 = 1$ ), the problem is centrally symmetric, hence the solution (23)–(25) for  $x > 0$  holds also for  $x < 0$ . As seen in Fig. 3(b), the respective interface height  $\eta(x/t)$  is double valued. This implies that the actual solution has to contain a jump.

Let us first consider  $x > 0$  and find the jump connecting solutions (24,25) with the downstream state where  $\eta_+ = -1$  and  $\vartheta_+ = 0$ . Substituting these downstream parameters

into the jump conditions (15,16), after a few rearrangements, we obtain

$$\vartheta^2 = 1 - \frac{2(1-\alpha)\eta}{\eta^2 + 2(\eta + \alpha) - 1}, \quad (27)$$

$$\dot{\xi} = \frac{1}{2}(1-\eta)\vartheta, \quad (28)$$

while Eqs. (24, 25) yield

$$\vartheta^2 = 1 - \eta^2. \quad (29)$$

There are only two possible interface heights,  $\eta = -1$  and  $\eta = 0$ , which satisfy Eqs. (27)–(29). The former corresponds to the continuous double-valued solution whereas the latter corresponds a jump spanning the lower half of the channel. The possible shear velocities and the respective propagation speeds for this jump, which are defined respectively by Eqs. (27,28), are  $\vartheta = \pm 1$  and  $\dot{\xi} = \pm \frac{1}{2}$ . The downstream direction of propagation corresponds to the positive solution. The velocity of propagation being independent of  $\alpha$  implies that this jump conserves not only the mass and impulse but also the circulation and energy.<sup>27</sup>

For the full lock exchange, there is a centrally symmetric upstream jump at  $x < 0$ , which spans the upper half of the channel from  $\eta = 0$  to  $\eta = 1$  and moves leftward at the velocity  $\dot{\xi} = -\frac{1}{2}$  (see Fig. 3b). This exact fully-conservative solution coincides with that assumed by Yih and Guha<sup>34</sup> but differs from the numerical solution obtained by Klemp, Rotunno, and Skamarock<sup>6</sup> which will be considered later in connection with the possible instability of deep gravity currents.<sup>27</sup>

Let us now consider a partial lock exchange with the upstream interface height  $\eta_0 = \sin(\frac{\pi}{2} - \theta_0)$ , where  $0 \leq \theta_0 \leq \pi$ . This initial state with  $\eta = \eta_0$  and  $\vartheta = 0$  corresponds to the angular variables  $\theta = \frac{\pi}{2} - \theta_0$  and  $\phi = 0$ . Then the positive Riemann invariant takes the form

$$r^+ = \theta + \phi = \frac{\pi}{2} - \theta_0,$$

from where we have  $\phi = \frac{\pi}{2} - \theta_0 - \theta$ . Using this relation, the negative Riemann invariant associated with the  $C^-$  characteristics, which extend upstream from the lock, can be written as

$$r^- = \phi - \theta = \frac{\pi}{2} - \theta_0 - 2\theta.$$

Since the respective characteristic velocity (21)

$$\lambda^- = -\frac{3}{4} \sin(2\theta + \theta_0) + \frac{1}{4} \sin \theta_0 \quad (30)$$

is constant along  $C^-$ , these characteristics are straight lines with the slope  $\lambda^- = \frac{x}{t}$ . Consequently, the solution can be written parametrically as follows:

$$\frac{x}{t} = -\frac{3}{4} \sin(2\theta + \theta_0) + \frac{1}{4} \sin \theta_0, \quad (31)$$

$$\eta^- = \sin \theta, \quad (32)$$

$$\vartheta^- = \cos(\theta + \theta_0). \quad (33)$$

To determine the range of applicability of this solution, we need to consider also the  $C^+$  characteristics. The slope of these characteristics varying across the  $C^-$  as follows

$$\lambda^+ = \frac{3}{4} \sin \theta_0 - \frac{1}{4} \sin(2\theta + \theta_0) = \frac{1}{3} \lambda^- + \frac{2}{3} \sin \theta_0. \quad (34)$$

becomes equal at  $\theta = -\theta_0$  to that of  $C^-$  :  $\lambda^+ = \lambda^- = \sin \theta_0 \geq 0$ . At this point, both families of characteristics become parallel to each other. It means that the applicability of solution (31)–(33) is limited to  $-\theta_0 \leq \theta \leq \frac{\pi}{2} - \theta_0$ . Equation (34) defining the  $C^+$  characteristics can be written in terms of  $x$  and  $t$  as follows

$$\frac{dx}{dt} = \frac{1}{3} \frac{x}{t} + \frac{2}{3} \sin \theta_0.$$

The general solution of this equation is  $x(t) = ct^{1/3} + t \sin \theta_0$ , where  $c$  is an unknown constant. The latter can be determined by matching this solution with that for the undisturbed upstream state  $x(t) = x_0 + \frac{1}{2}t \sin \theta_0$ , which holds below the leftmost  $C^-$  characteristic defined by

$$\frac{x}{t} \leq \min \lambda^- = \frac{1}{3} \sin \theta_0 - \frac{4}{3}.$$

Both families of characteristics for the upstream region are shown in Fig. 2(b).

Downstream from the lock ( $x > 0$ ), where the initial state is the same as for the full lock exchange, solution remains defined by Eqs. (23)–(25), which hold for  $-\frac{\pi}{2} \leq \theta < 0$ . Note that for  $\theta_0 > 0$ , solution (31)–(33) extends downstream up to  $\frac{x}{t} = \sin \theta_0$ , which corresponds to  $\theta = -\theta_0$  in Eq. (31). Thus, this solution overlaps with that defined by Eqs. (23)–(25) in the sector  $0 \leq \frac{x}{t} \leq \sin \theta_0$ . As usual, the double-valuedness of this solution implies the presence of a jump.

Let us first consider the jump connecting the upstream state  $\eta = \eta_0$  and  $\vartheta = 0$  with solution (31)–(33). Substituting solution (32,33) into the jump conditions (15,16), we obtain:

$$\vartheta^2 = \frac{(\eta_0 - \eta)^2(\eta_0 + \eta + 2\alpha)}{(1 - \eta^2)(\eta_0 - \eta) + 2(\eta + \alpha)(1 - \eta_0\eta)} = \left( \eta_0 \sqrt{1 - \eta^2} - \eta \sqrt{1 - \eta_0^2} \right)^2. \quad (35)$$

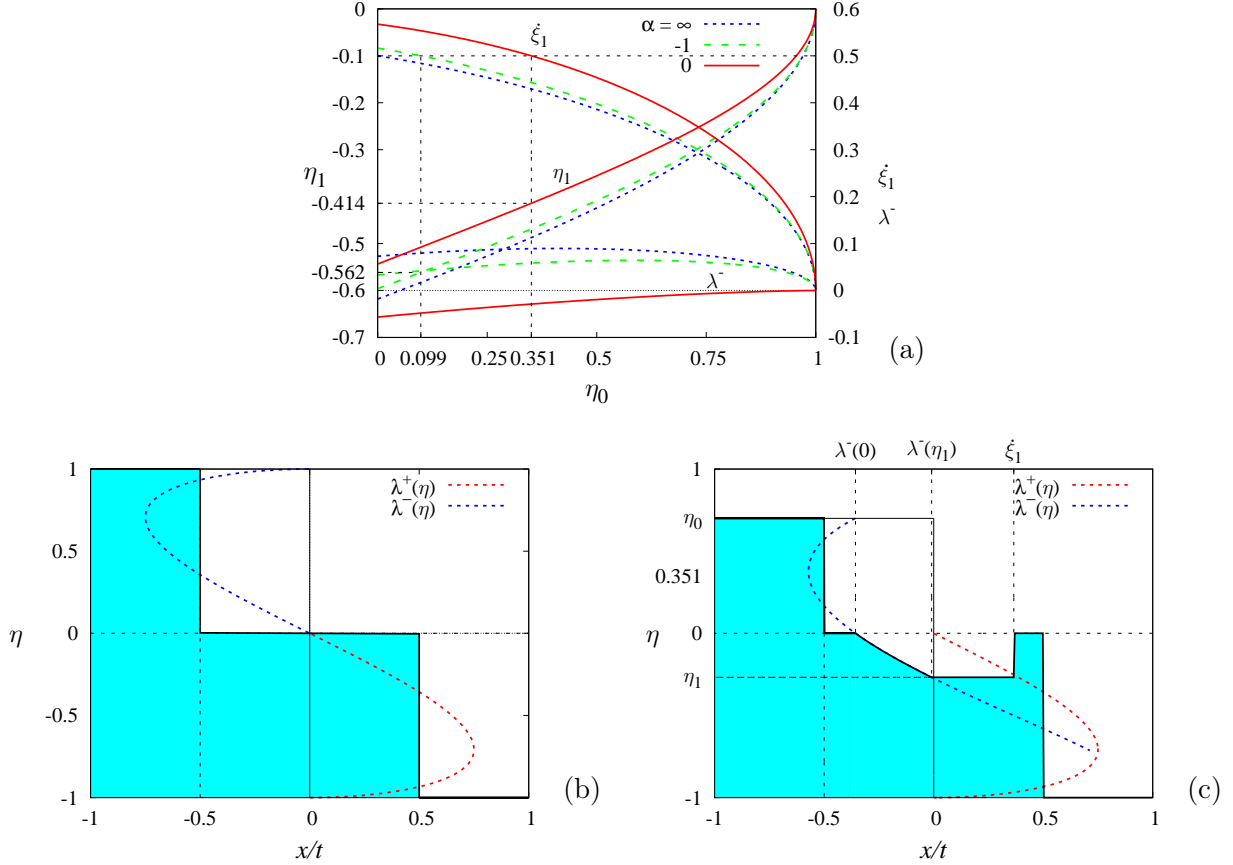


Figure 3. The interface height  $\eta_1$ , the velocity of propagation  $\dot{\xi}_1$  of the jump trailing the head-block and the characteristic velocity  $\lambda^-$  at  $\eta = \eta_1$  versus the upstream interface height  $\eta_0$  (a); the interface height versus the similarity variable  $x/t$  for the full lock exchange:  $\eta_0 = 1$  (b) and partial lock exchange:  $\eta_c < \eta_0 < 1$ , where  $\eta_c = 0.099$  is defined by Eq. (38).

This equation has only two roots:  $\eta = \eta_0$  and  $\eta = 0$ . As for the full lock exchange, the first root corresponds to the original continuous solution, which however is double valued if  $\eta_0 > 0$ . The second root describes a jump from  $\eta = \eta_0$  to the channel mid-height  $\eta = 0$ . The shear velocity behind this jump and its velocity of propagation, which are defined respectively by Eqs. (35) and (15), are  $\vartheta = \eta_0$  and  $\dot{\xi} = -\frac{1}{2} \frac{\vartheta}{\eta_0} = -\frac{1}{2}$ . The fact that  $\dot{\xi}$  is independent of  $\eta_0$  as well as of  $\alpha$  implies that this jump is fully conservative and, thus, represents a long-wave approximation to the so-called solibore which appears in the non-hydrostatic model.<sup>27</sup>

In the downstream direction, the uniform state behind this jump  $(\eta, \vartheta) = (0, \eta_0)$  connects with the solution (31)–(33) at the point  $\theta = 0$ . According to Eq. (31), this point moves at the

velocity  $\frac{x}{t} = -\frac{1}{2} \sin \theta_0 \leq -\frac{1}{2}$ , which does not exceed the velocity of the upstream jump. At larger distances  $x/t$ , the interface, which is defined parametrically by Eqs. (31,32), descends below the mid-height  $\eta = 0$ . This solution can be connected with the solution downstream from the lock which, as noted above, is the same as that for the full lock exchange:  $\eta_+ = 0$  and  $\vartheta_+ = 1$ . With this front state, the jump conditions (15,16) yield the following relationship between  $\vartheta_- = \vartheta_1$  and  $\eta_- = \eta_1$  behind the jump:

$$\vartheta_1 = \frac{(2\alpha + \eta_1)(1 - \eta_1^2)}{2\alpha + \eta_1(1 + \eta_1^2)}.$$

Substituting solution (32,33) into this equation, we obtain

$$\vartheta_1 = \cos(\theta_1 + \theta_0) = \frac{(2\alpha + \sin \theta_1)(1 - \sin^2 \theta_1)}{2\alpha + \sin \theta_1(1 + \sin^2 \theta_1)}, \quad (36)$$

which relates  $\theta_1$  behind the jump with the corresponding upstream quantity  $\theta_0 = \arccos \eta_0$ . This equation is solvable analytically for  $\theta_0$  in terms of  $\theta_1$  or numerically the other way round. The analytical solution  $\eta_1 = \sin \theta_1$  for the interface height behind the jump and its velocity of propagation

$$\dot{\xi}_1 = -\frac{\eta_1(3 - \eta_1^2)}{2(1 + \eta_1^2)} \quad (37)$$

as well as the characteristic velocity  $\lambda^-(\eta_1)$  are plotted in Fig. 3(a) against the upstream interface height  $\eta_0$ . As seen in Fig. 3(c),  $\lambda^-(\eta_1)$  defines the upstream limiting point of the flat depressed interface region which forms behind the head block with the trailing edge advancing at a supercritical velocity  $\dot{\xi}_1 > \lambda^-(\eta_1)$ . Figure 3(a) shows that  $\dot{\xi}_1$  increases with decreasing  $\eta_0$  and attains the velocity of the leading head block edge  $\dot{\xi} = 0.5$  at

$$\eta_c \approx 0.351, 0.099, 0 \quad \text{for} \quad \alpha = 0, -1, \infty. \quad (38)$$

At this critical point, both edges merge and, thus, the head block vanishes. It means that for  $\eta_0 \leq \eta_c$ , solution (31)–(33) has to connect directly to the quiescent downstream state with  $\eta_+ = -1$  and  $\vartheta_+ = 0$ . Then the interface height and the shear velocity behind the jump are related by Eq. (27). Combining this relation with solution (32,33), we obtain

$$\vartheta_1 = \cos(\theta_1 + \theta_0) = \left( \frac{\cos^2 \theta_1 - 2\alpha(1 + \sin \theta_1)}{\cos^2 \theta_1 - 2(\alpha + \sin \theta_1)} \right)^{1/2}. \quad (39)$$

Similar to Eq. (36), this equation is solvable analytically for  $\theta_0$  in terms of  $\theta_1$  or numerically the other way round. The speed of propagation  $\dot{\xi}$  is obtained by substituting  $\eta_1 = \sin \theta_1$  and  $\vartheta_1$  found by solving this equation for  $\eta$  and  $\vartheta$  in Eq. (28).

The downstream jump parameters defined by Eq. (39) are plotted in Fig. 4(a) for the whole range of upstream heights which, in principle, admit this type of solution without the head block. The overall interface height versus the similarity variable  $x/t$  is shown in Figs. 4(b,c). As seen, there are two different interface configurations possible in this case. The first configuration, which is shown in Fig. 4(b), corresponds to  $0 \leq \eta_0 \leq \eta_c$  and features an upstream jump from  $\eta_0$  to the mid-height  $\eta = 0$  as in the case with the head block. The second configuration corresponding to  $\eta_0 \leq 0$ , which is shown in Fig. 4(c), has no upstream jump. In the latter case, the upstream state connects directly to solution (32,33) at  $\eta = \eta_0$ , which is the other root of Eq. (35).

It is important to note that for  $\eta_0 \leq 0$ , solution (32,33) can in principle connect directly to the downstream state  $\eta = -1$  at  $\theta = -\frac{\pi}{2}$  without a leading jump, as in the dam-break solution for the single-layer case. The following considerations, however, imply that, in the two-layer case, this alternative solution is inherently unstable. Namely, as seen in Fig. 4(b,c), the sharp edge in the continuous solution propagates with a non-zero characteristic velocity  $\lambda^-$  which is defined by Eq. (30) with  $\theta = -\pi/2$  corresponding to  $\eta = -1$ . Now consider a perturbation resulting in a small non-zero edge height. As it may be seen in Fig. 4(a), the speed of propagation  $\dot{\xi}$  for jump of finite height drops to zero in this limit. This effectively halts the propagation of the edge causing its height to increase further as long as the fluid behind it moves faster than the edge. As a result, the edge acquires a finite height. This is confirmed by the subsequent direct numerical solution. A similar mechanism can be behind the formation of the elevated head block when  $\eta_0 > \eta_c$ .

For a thin bottom layer with  $h_0 = \frac{1}{2}(1 + \eta_0) \rightarrow 0$ , Eq. (39) can be solved explicitly as follows

$$\theta_1 + \pi/2 \approx (\pi - \theta_0)/(1 + 1/\sqrt{2}).$$

Using the above result, we readily recover the solution for the single-layer dam-break problem with the reduced gravity and von Kármán front condition:  $\dot{\xi}_1 = \sqrt{2h_1}$  and  $\lambda^+ = (\sqrt{2}-1)\sqrt{h_1}$ , where  $h_1 = 2(\sqrt{2}-1)^2 h_0 \approx 0.343h_0$  is the downstream front height.<sup>23</sup> (Sec. 2.5) As noted above, a finite front height is caused by the instability of the sharp edge in the two-layer dam-break solution.

To conclude this section let us note that the existence of analytical expressions for the Riemann invariants used above is advantageous but not crucial for solving the problem since

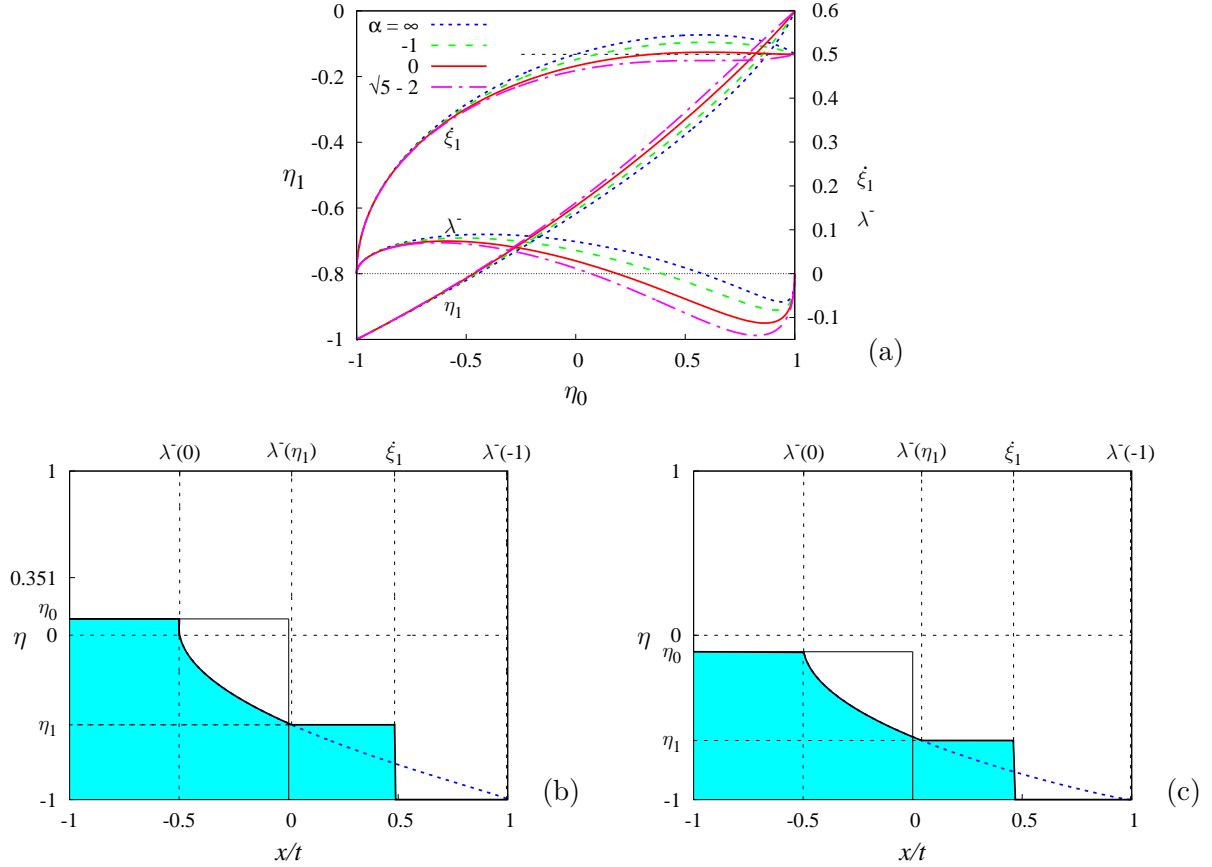


Figure 4. The interface height and the velocity of propagation of the leading jump (a) and the overall interface shape for the partial lock exchange with  $0 \leq \eta_0 \leq 0.351$  (b) and  $\eta_0 \leq 0$  (c).

the characteristic equation (14) can also be integrated numerically as done, for example, by Klemp, Rotunno, and Skamarock<sup>6</sup> and Khodkar, Nasr-Azadani, and Meiburg<sup>25</sup> using the long form of this equation.<sup>17</sup> In this case, the uniform initial states downstream and upstream of the lock,  $\vartheta|_{\eta=-1} = 0$  and  $\vartheta|_{\eta=\eta_0} = 0$ , provide boundary conditions for Eq. (14). Since this equation represents two first-order ordinary differential equations defined by the plus and minus signs at the second term, only one boundary condition is required for each equation. Because the sign in Eq. (14) determines the direction of flow, it depends on which side from the lock gate the heavier fluid is contained. For the configuration considered in this study with the heavier fluid contained on the left, the downstream and upstream boundary conditions apply to Eq. (14) with the plus sign and minus signs, respectively.



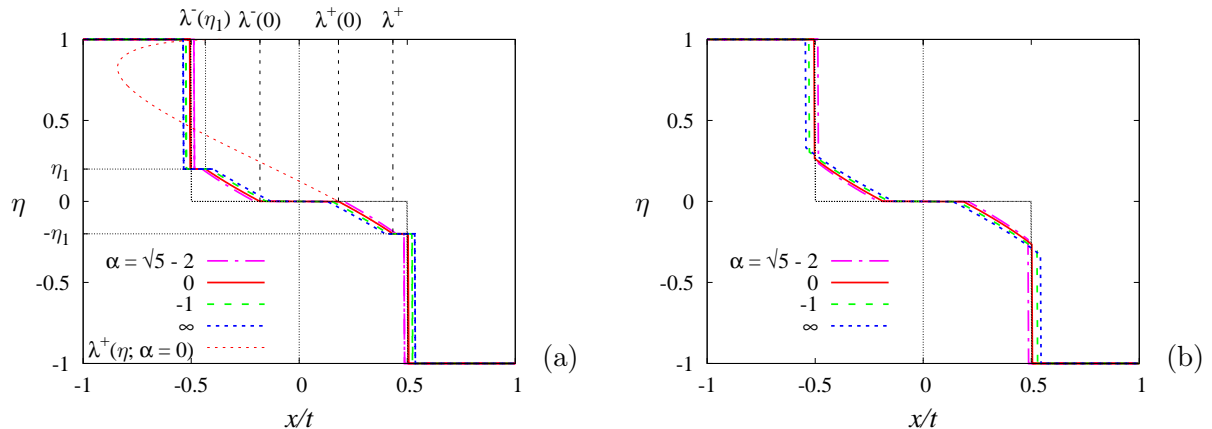


Figure 5. The interface height in the modified lock-exchange problem for various  $\alpha$  with the upstream and downstream gravity current heights fixed to  $\eta_0 = \pm 0.2$  (a) and with the lowest possible gravity current height for each  $\alpha$  (b).

#### IV. LOCK EXCHANGE WITH A MODIFIED INITIAL STATE

As already noted, the solution found above differs from the previously obtained numerical solution.<sup>6</sup> The difference is due to the non-standard method of characteristics used by Klemp, Rotunno, and Skamarock<sup>6</sup> who employ Benjamin's front condition directly as a boundary condition for the characteristic equation. In the conventional simple-wave approach used in the previous section, it is the quiescent downstream state which defines the relevant boundary condition. The front condition, in turn, is used to eliminate multi-valued parts of the solution, if any, by fitting in the jumps. These two approaches are not equivalent and lead to different results because they describe different physical problems.

Using the front condition as a boundary condition is equivalent to assuming the initial downstream state to be a gravity current rather than a quiescent fluid as in the original lock-exchange problem. Such an assumption may be justified if the loss of hyperbolicity or instability breaks the dependence of the solution on the initial state. In this case, one can expect a stable gravity current of a lower height to form as the effective downstream state. Although the height of this gravity current is not uniquely defined, the problem can still be solved analytically in a similar way to the original lock-exchange problem in the previous section. For the sake of completeness, in this section, we present also an analytical solution of this alternative formulation.

Following Klemp, Rotunno, and Skamarock<sup>6</sup>, we now assume the downstream state to be a gravity current with the interface height  $\eta_1$  and the shear velocity  $\vartheta_1(\eta_1) \geq 0$  defined by Eq. (27). Then the negative Riemann invariant (20), which is constant along the characteristics propagating upstream from this uniform state, can be written as follows

$$r^- = \phi - \theta = \arcsin \vartheta_1(\eta_1) - \arcsin \eta_1. \quad (40)$$

Rearranging this expression as  $\phi = r^- + \theta$ , the positive Riemann invariant can be written as follows

$$r^+ = \phi + \theta = r^- + 2\theta.$$

Since both  $r^-$  and  $r^+$  are constant along the  $C^+$  characteristics, which propagate into the downstream state, so is also the associated characteristic velocity (21)

$$\lambda^+ = \frac{3}{4} \cos r^+ - \frac{1}{4} \cos r^-.$$

Then the solution can be written in the parametric form as follows

$$\frac{x}{t} = \frac{3}{4} \cos(r^- + 2\theta) - \frac{1}{4} \cos r^-, \quad (41)$$

$$\eta^+ = \sin \theta, \quad (42)$$

$$\vartheta^+ = \sin(r^- + \theta), \quad (43)$$

where  $\eta \geq \eta_1$  and  $r^-$  depends on  $\eta_1$  as defined by Eq. (40). For the full lock exchange, the symmetry of the problem implies:  $\{\eta, \vartheta\}(-x/t) = \{-\eta, \vartheta\}(x/t)$ . It means that the upstream and downstream solutions connect at  $\eta = 0$  without a jump, as shown in Fig. 5(a) for  $\eta_1 = -0.2$  and various  $\alpha$ . For such a solution to be possible, the gravity current cannot propagate slower than the downstream characteristic velocity for the respective height:  $\dot{\xi}(\eta_1) \geq \lambda^+(\eta_1)$ , where the latter defines the speed at which the lower point of the sloped part of the interface moves. This, in turn, implies that the height of gravity current  $\eta_1$  cannot be lower than the critical value  $\eta_c$  which is defined depending on  $\alpha$  by  $\dot{\xi}(\eta_c) = \lambda^+(\eta_c)$ . As seen in Fig. 6,  $\eta_c$  coincides with the point at which  $\dot{\xi}(\eta_1)$  attains maximum for a given  $\alpha$  provided that  $\alpha < \alpha_c = \sqrt{5} - 2$ .<sup>27</sup> If  $\alpha$  exceeds  $\alpha_c$ , the critical height  $\eta_c$  switches from the maximum to the minimum of  $\dot{\xi}$ . The latter emerges at  $\eta = -\alpha$  when  $\alpha$  becomes greater than zero and descends towards the maximum with the increase in  $\alpha$ . At  $\alpha = \alpha_c$ , both stationary points

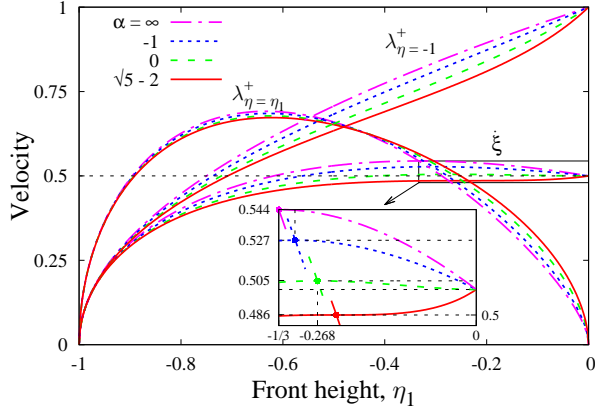


Figure 6. The characteristic downstream wave speed  $\lambda^+$  at the top ( $\eta = \eta_1$ ) and bottom ( $\eta = -1$ ) of the gravity current and the front velocity  $\dot{\xi}$  versus the front height for  $\alpha = \infty, -1, 0, \sqrt{5} - 2$ .

merge forming an inflection point. As a result, the front velocity  $\dot{\xi}$  becomes a monotonically increasing function of  $\eta_1$  at this particular value of  $\alpha$ . If  $\alpha$  exceeds  $\alpha_c$ , the inflection points splits into two stationary points: a maximum located at  $\eta_c = -\alpha$  and minimum moving back towards the mid-plane  $\eta = 0$  which it reaches at  $\alpha = \frac{1}{2}$ .

The considerations above imply that if the initial height of gravity current  $\eta_1$  is lower than  $\eta_c$ , the fluid beneath the sloped interface would run over the front until its height reaches  $\eta_c$  for a given  $\alpha$ . The highest possible  $\eta_c$  is attained at  $\alpha = \alpha_c$ . It is because for  $\alpha > \alpha_c$  the critical height  $\eta_c$  switches to the local minimum of  $\dot{\xi}$  but the latter is expected to be unstable.<sup>15,35</sup> Namely, a virtual perturbation decreasing the front height would increase the front speed. Then the mass conservation would enhance the initial perturbation and, thus, cause the gravity current collapse to a lower depth. Therefore,  $\eta_c = -\alpha_c$  is the highest possible value of  $\eta_c$ . The corresponding front velocity  $\dot{\xi} = \alpha_c^{1/2} \approx 0.486$  can be seen in Fig. 7 to agree very well with the highly accurate numerical results of Härtel, Meiburg, and Necker<sup>36</sup> for the gravity currents generated by the lock exchange with free-slip boundary conditions. The other values of  $\alpha$  produce noticeable higher front velocities. With real no-slip boundary conditions, a much higher Reynolds number seems to be required to achieve this inviscid limit.

The solution obtained above can easily be extended to the partial-height lock exchange where the upstream state is a layer of quiescent fluid with the interface located at  $\eta = \eta_0$ . In

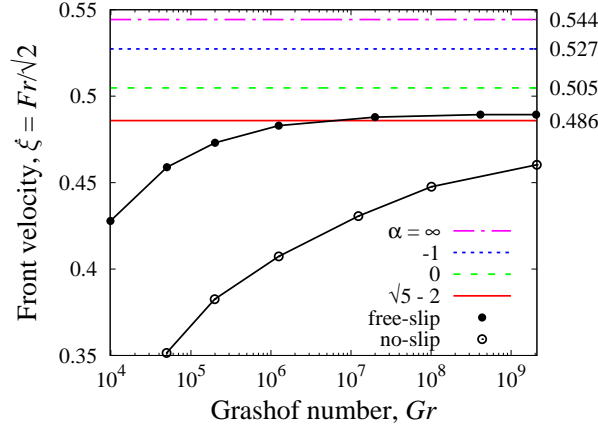


Figure 7. Comparison of critical gravity current speeds for various  $\alpha$  with the numerical results of Härtel, Meiburg, and Necker<sup>36</sup> for gravity currents generated by the lock exchange with free-slip and no-slip boundary conditions. The conversion factor of  $1/\sqrt{2}$  is due to the channel half-height used as the length scale in the definition of Froude number  $Fr$  by Härtel, Meiburg, and Necker<sup>36</sup>. The Grashof number defines the magnitude of the driving force which produces characteristic flow velocity with the Reynolds number  $Re \sim \sqrt{Gr}$ .

this case, the initial upstream state is supposed to contain a bore with the interface height  $\eta_1 \leq \eta_0$  and the shear velocity  $\vartheta_1(\eta_0, \eta_2)$  which is defined by the LHS of Eq. (35) with  $\eta_1$  standing instead of  $\eta$ . By the same arguments as before, we find that solution is described by Eqs. (31)–(33) with  $\theta_0 = \frac{\pi}{2} - r^+$ , where

$$r^+ = \phi + \theta = \arcsin \vartheta_1(\eta_0, \eta_1) + \arcsin \eta_1 \quad (44)$$

is the positive Riemann invariant corresponding to the upstream bore.

The lowest possible bore height  $h_1 = (1 + \eta_1)/2$ , which is determined by the corresponding characteristic velocity becoming equal with the maximal front velocity for a given  $\alpha$ , is plotted in Fig. 8(a) against the lock height  $h_0$  for various  $\alpha$ . For  $\alpha > 0$ , the energy constraint (17), which can be written as follows

$$\dot{\epsilon} = \frac{\eta_1 (\alpha - \eta_0) (1 - \eta_1^2) (\eta_0 - \eta_1)^3 \sqrt{2\alpha - \eta_0 - \eta_1}}{(3\eta_0\eta_1^2 - \eta_1^3 + 2\alpha(1 - \eta_0\eta_1) - \eta_1 - \eta_0)^{3/2}},$$

permits such upstream bores only for  $\eta_0 \geq 2\alpha$ . This constraint can be relaxed by assuming  $\alpha$  to vary depending on  $\eta_0$  so as to minimize the maximum of propagation velocity for a given  $\eta_0$ . As before, this happens when the maximum of  $\dot{\epsilon}$  merges with the minimum

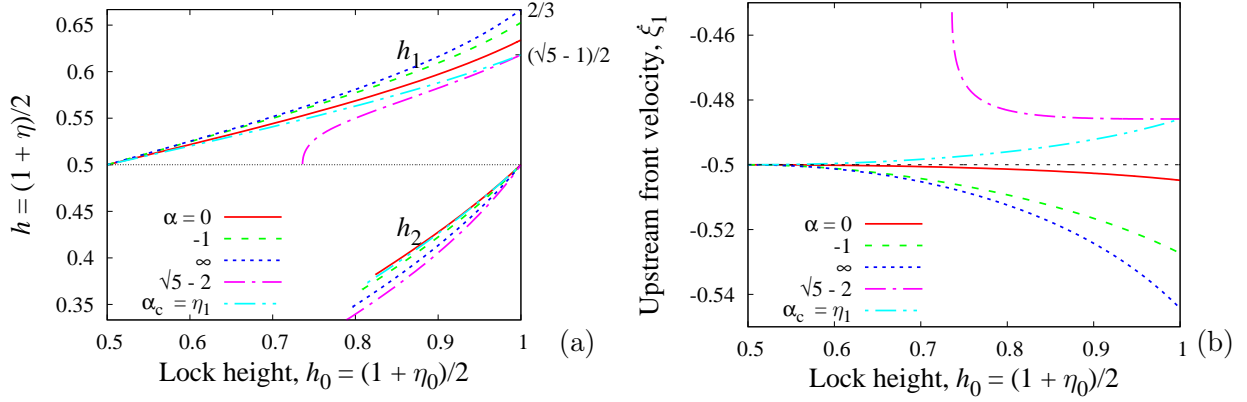


Figure 8. The interface height  $h_1$  that produces the highest stable bore, the intermediate interface height  $h_2$  (a) and the respective propagation velocity (b) against the lock height  $h_0$  for various  $\alpha$ .

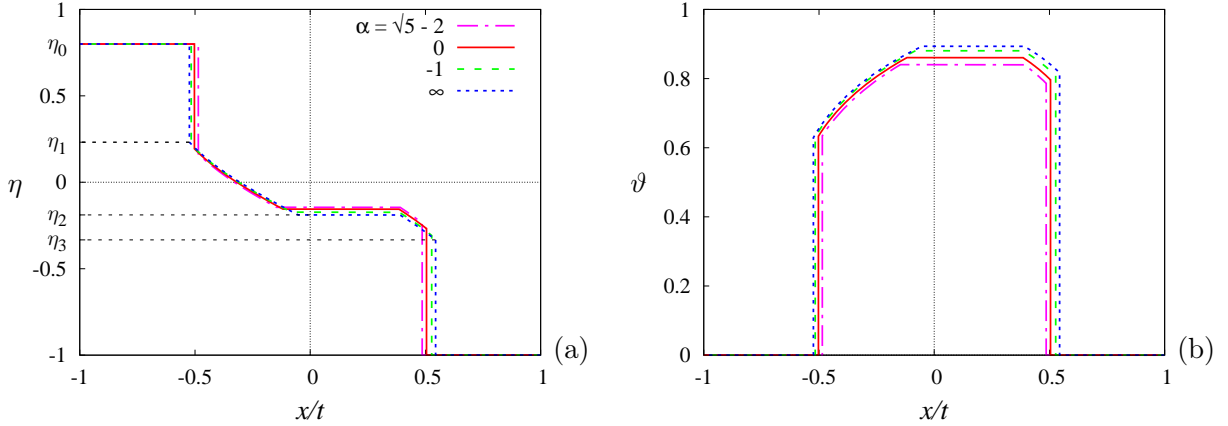


Figure 9. The interface height in the modified partial lock-exchange flow (a) and the corresponding shear velocity (b) for the lock height  $h_0 = (1 + \eta_0)/2 = 0.9$ .

forming a stationary inflection point at  $\eta_1 = \alpha \geq 0$ . The solution of  $\partial_{\eta_1}^2 \dot{\xi}(\eta_0, \eta_1; \alpha) \Big|_{\eta_1 = \alpha} = 0$  defining this critical point, which can be found analytically but not presented here due to its complexity, is plotted in Fig. 8(a).

As for the full lock exchange, the upstream and downstream solutions connect without jump at the point of equal shear velocities  $\vartheta_+ = \vartheta_-$  (see Fig. 9). This yields  $\theta_2 = (r^+ - r^-)/2$  with the Riemann invariants defined by Eqs. (40,44). The corresponding interface height  $h_2 = (1 + \eta_2)/2$ , where  $\eta_2 = \sin((r^+ - r^-)/2)$ , is plotted in Fig. 8(a) against the lock height  $h_0$ .

The above solution holds only for sufficiently high locks which produce an intermediate interface height  $\eta_2$  not lower than the downstream front height  $\eta_3$  for a given  $\alpha$ . For lower locks, the upstream solution can connect directly to the quiescent downstream state. The downstream front heights and velocities resulting from the jump condition for various  $\alpha$  are plotted in Fig. 10 along with the solution of the original lock-exchange problem. This figure also shows the relevant numerical and experimental results. As seen, the difference between the modified and original lock-exchange solutions is significant only for the fronts of supercritical height. Note that this is the height at which the front speed for a given  $\alpha$  attains maximum. The height of gravity current predicted by the SW model can be seen to agree well with the DNS results of Khodkar, Nasr-Azadani, and Meiburg<sup>25</sup> while the experimental results of Shin, Dalziel, and Linden<sup>7</sup> for shallow locks ( $h_0 \lesssim 0.5$ ) are somewhat higher and close to the half lock height predicted by their theoretical model. It is also interesting to note that the DNS results of Khodkar, Nasr-Azadani, and Meiburg<sup>25</sup> feature a gravity current head which is present for tall locks ( $h_0 > 0.5$ ) and extends up to the channel mid-height as predicted by the SW solution.

## V. NUMERICAL SIMULATION USING CONSERVATIVE SW EQUATIONS

In this section, we verify the analytical solution obtained in Sec. III by solving the ideal lock-exchange problem numerically using the SW mass and generalized momentum conservation equations (7,10) and the LWLF4 composite scheme in which three steps of Lax-Wendroff scheme are followed by a step of Lax-Friedrichs scheme.<sup>37</sup> This composition significantly reduces numerical oscillations around the jumps, which are typical to the Lax-Wendroff scheme, without introducing excessive numerical diffusion, which is typical to the Lax-Friedrichs scheme. The generalized momentum equation (10) is solved for  $\alpha = 0, -1, 10^{10}$ , where the last value effectively reduces the momentum equation to the circulation conservation equation (6) which is formally recovered in the limit  $\alpha \rightarrow \infty$ .

It is important to note that the integration of Eq. (10) is hindered by the product  $(\eta + \alpha)\vartheta = w$  which appears as a dynamical variable. This quantity has to be determined along with  $\eta$  in each time step and then used to calculate the shear velocity as  $\vartheta = w/(\eta + \alpha)$ .

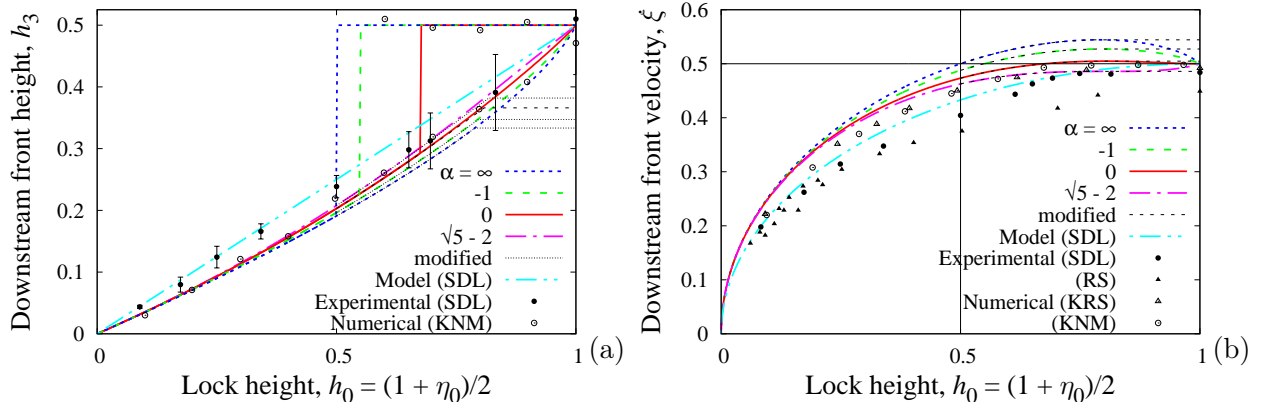


Figure 10. The front height (a) and velocity of the downstream gravity current (b) for various  $\alpha$  against the lock height: comparison of the modified and original lock-exchange solutions with the experimental results of Shin, Dalziel, and Linden (SDL)<sup>7</sup> and Rottman and Simpson (RS)<sup>17</sup>; the numerical results of Klemp, Rotunno, and Skamarock (KRS)<sup>6</sup> and Khodkar, Nasr-Azadani, and Meiburg (KNM)<sup>25</sup>; the model of Shin, Dalziel, and Linden (SDL)<sup>7</sup>. The abrupt variation of the front height in the original lock-exchange solution is due to the disappearance of the head block at the critical upstream interface height (38).

The division by  $\eta + \alpha$  in the last step can produce large numerical errors at the points where  $\eta$  happens to be close to  $-\alpha$ , which is possible when  $|\alpha| < 1$ . Although this numerical uncertainty can formally be resolved using the L'Hôpital's rule, it was not possible to construct a stable numerical scheme in this way. Since there is no such a problem in the circulation conservation equation (6) and the latter is equivalent to the momentum equation at smooth parts of the interface, the division by zero was avoided by adopting a hybrid approach in which Eq. (6) is used instead of Eq. (10) at the grid points where  $|\eta + \alpha| < \varepsilon \approx 10^{-3}$  to find  $\vartheta$  directly. This approach was found to produce numerical results in good agreement with the analytical solution for a range of lock heights (see Fig. 11).

First, as seen in Fig. 11(a), the exact solution for the full lock-exchange is reproduced using equal time and space steps. This is an optimal choice which renders the scheme marginally stable and ensures that the front advances one grid step in one time step. In general, such marginally stable schemes are known to reduce spurious oscillations at the jumps.<sup>38</sup> The scheme becomes unstable at larger time steps which violate the Courant-

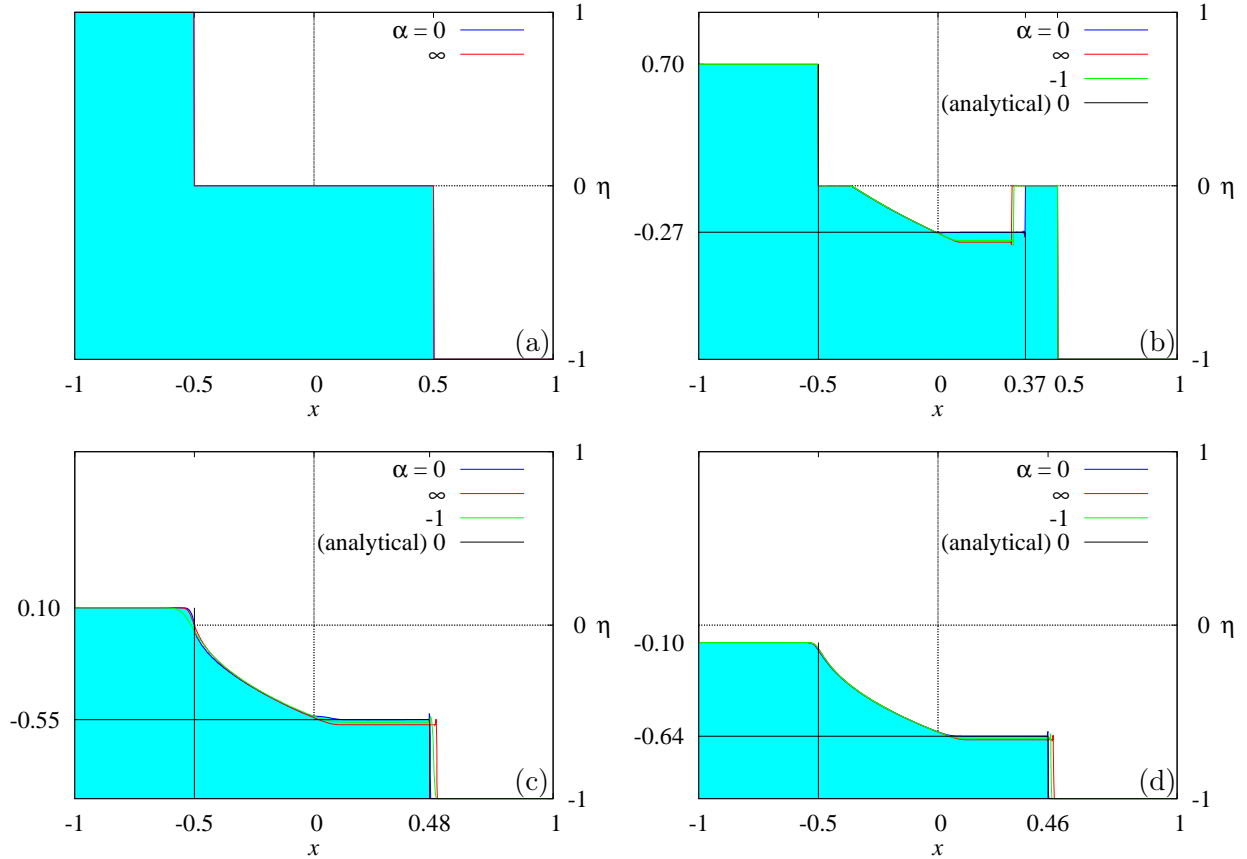


Figure 11. The interface height at the time instant  $t = 1$  after opening the lock gate of height  $\eta_0 = 1$  (a), 0.7 (b), 0.1(c) and  $-0.1$ (d) computed numerically by solving the SW mass and generalized momentum conservation equations (7,10) with  $\alpha = 0$  (filled area),  $-1$  and  $\infty$  using the LWLF4 scheme with the time step  $\tau = 10^{-3}$  and the spatial step  $\delta = 10^{-3}$  (a,b) and  $\tau = 2.5 \times 10^{-4}$ ,  $\delta = 1.25 \times 10^{-4}$  (c,d).

Friedrichs-Lewy condition, whereas spurious oscillations arise at smaller time steps. In both cases, the numerical solution for the full lock-exchange breaks down.

Using the same time step and grid size as for the full lock-exchange, we were able to reproduce the exact solution also for a range of partial lock-exchange flows. The numerical solutions for the lock height  $\eta_0 = 0.7$  is shown in Fig. 11(b) for  $\alpha = 0, -1, \infty$  along with the key parameters of the analytical solution for  $\alpha = 0$ . In this case, spurious oscillations appear behind the head block because the trailing jump advances less than one grid step per time step. As the head block becomes progressively thinner with lowering  $\eta_0$ , there is



a range lock heights  $0.1 \lesssim \eta_0 \lesssim 0.7$  for which it was not possible to find a numerically stable solution. The stable numerical solution that re-emerges at  $\eta_0 \approx 0.1$  has no head block but just the downstream and upstream jumps. The latter can be seen in Fig. 11(c) to be somewhat smoothed out by the numerical diffusion produced by the Lax-Friedrichs step of the LWLF4 scheme. This upstream jump vanishes when the lock is lower than channel mid-height ( $\eta_0 \leq 0$ ). The corresponding numerical solution shown in Fig. 11(c) can be seen to produce a finite front height as predicted by the analytical solution. It is important to note that in this case, also a smooth analytical solution akin to the single-layer dam-break solution is in principle possible. However, as argued above, such a smooth solution is unstable and, thus, not observable in the numerical solution.

## VI. SUMMARY AND CONCLUSION

In the present paper, we considered the lock-exchange flow which is triggered by rapidly removing a vertical gate between two fluids of slightly different densities contained in a horizontal channel bounded by a rigid lid. Using the method of characteristics and analytic expressions for the Riemann invariants of the underlying system of two hyperbolic differential equations, we obtained a simple-wave solution for this problem. The multivaluedness as well as the instability of the solution was found to result in a number of hydraulic jumps which were resolved using the conservation of mass and impulse (pseudo-momentum). The respective Rankine-Hugoniot jump conditions contain a free parameter  $\alpha$ , which defines the relative contribution of each layer to the pressure gradient along the interface in the generalized SW momentum equation.<sup>27</sup> We considered the solution for  $\alpha = 0$ , which corresponds to the interfacial pressure gradient determined by both layers with equal weight coefficients, along with the solutions for  $\alpha = -1$  and  $\alpha \rightarrow \infty$  which reproduce the classic front condition of Klemp, Rotunno, and Skamarock<sup>28</sup> and the circulation conservation condition of Borden and Meiburg<sup>39</sup>.

For the full-height lock exchange, which corresponds to the heavier fluid behind the lock gate occupying the whole channel, the solution does not depend on  $\alpha$  and consists of a downstream gravity current and a symmetric upstream bore which span the upper and lower halves of the channel and propagate at the dimensionless speed (Froude number) equal to

1/2. This solution, which conserves not only the mass and impulse but also the circulation and energy, coincides with that assumed by Yih and Guha<sup>34</sup> but differs from the numerical solution obtained by Klemp, Rotunno, and Skamarock<sup>6</sup> who assume initial state to be a gravity current rather than a quiescent fluid.

The upstream part of the solution remains independent of  $\alpha$  also for partial-height lock exchange. The reduction of the lock height just reduces the upstream bore height which elevates above the channel mid-height and keeps propagating upstream at a constant speed  $-1/2$ . This bore, which is fully conservative as for the full lock-exchange, persists as long as the upstream interface is located above the channel mid-height. In this case, the downstream gravity current features an elevated head block which extends up to the channel mid-height. Both the upstream bore and the elevated downstream head are in a good agreement with the 2D DNS results of Khodkar, Nasr-Azadani, and Meiburg<sup>25</sup>.

The solution with the head block, however, is possible only for the upstream interface heights above a certain minimal height which depends on  $\alpha$ . The head block is connected to the interface depression behind it by a back-step-type jump whose speed of propagation increases with lowering the upstream interface height until, at a certain critical height depending on  $\alpha$ , it reaches the leading front speed  $1/2$ . At this critical point, the head block vanishes and the upstream solution connects directly to the quiescent downstream state.

Since the upstream state can connect directly to the quiescent downstream state without the head block also at larger upstream interface heights, multiple solutions are in principle possible. If the ensuing gravity current exceeds a certain critical height depending on  $\alpha$  at which its speed of propagation attains maximum, physical considerations imply that such a gravity current is unstable.<sup>27</sup> This instability can result in the increase in the height of gravity current up to the channel mid-height so giving rise to the elevated head which is observed also in the 2D DNS results.<sup>25</sup>

Alternatively, this instability may cause the front of a supercritical gravity current to collapse to a lower height corresponding to the maximal velocity of propagation for a given  $\alpha$ . Such a collapse could break the dependence of the solution on the initial conditions and thus to lead to a new initial state which contains a gravity current of lower depth. This assumption underlies the alternative formulation of the lock exchange problem which was also considered in this paper. Although the new front height is not uniquely defined,

the problem can be solved analytically using the method of characteristics. The resulting gravity current speed can exceed  $\frac{1}{2}$ , especially when the conservation of circulation with  $\alpha \rightarrow \infty$  or the momentum conservation with  $\alpha = -1$  are assumed. This result is at odds with experimental observations as well as with numerical simulations which show the front speed to be somewhat lower than  $\frac{1}{2}$ . A much better agreement with highly accurate numerical results is achieved by  $\alpha = \sqrt{5} - 2$ , which produces the largest stable front height and yields the front speed  $\dot{\xi} = \alpha^{1/2} \approx 0.486$ . This value of  $\alpha$  can be selected dynamically by the collapse of unstable gravity current stopping at at the largest possible front height.

The exact solution, which represents an inviscid approximation to high-Reynolds-number limit, can be used as a benchmark for SW numerical schemes. In the present paper, we demonstrated that two-layer SW equations for the mass and generalized momentum conservation can describe interfacial gravity waves containing hydraulic jumps in a self-contained way without invoking external closure conditions. This is a definite achievement as previously two-layer SW equations were thought to be inherently incomplete and requiring externally derived front conditions in order to describe hydraulic jumps.

## AUTHOR DECLARATIONS

### Conflict of Interest

The authors have no conflicts to disclose.

## REFERENCES

- <sup>1</sup>J. J. Stoker, *Water waves: The mathematical theory with applications* (Wiley, 1958).
- <sup>2</sup>R. S. Johnson, *A modern introduction to the mathematical theory of water waves* (Cambridge, 1997).
- <sup>3</sup>A. Barré de Saint-Venant, “Théorie et équations générales du mouvement non permanent des eaux courantes,” *Comptes Rendus des séances de l’Académie des Sciences, Paris, France*, Séance **17**, 147–154 (1871).
- <sup>4</sup>A. Ritter, “Die Fortpflanzung der Wasserwellen,” *Zeitschrift des Vereines Deutscher Ingenieure* **36**, 947–954 (1892).

- <sup>5</sup>J. E. Simpson and R. E. Britter, “The dynamics of the head of a gravity current advancing over a horizontal surface,” *J. Fluid Mech.* **94**, 477–495 (1979).
- <sup>6</sup>J. B. Klemp, R. Rotunno, and W. C. Skamarock, “On the dynamics of gravity currents in a channel,” *J. Fluid Mech.* **269**, 169–198 (1994).
- <sup>7</sup>J. O. Shin, S. B. Dalziel, and P. F. Linden, “Gravity currents produced by lock exchange,” *J. Fluid Mech.* **521**, 1–34 (2004).
- <sup>8</sup>M. B. Abbott, “On the spreading of one fluid over another,” *La Houille Blanche* **6**, 827–856 (1961).
- <sup>9</sup>E. H. Fyhn, K. Y. Lervåg, Å. Ervik, and Ø. Wilhelmsen, “A consistent reduction of the two-layer shallow-water equations to an accurate one-layer spreading model,” *Phys. Fluids* **31**, 122103 (2019).
- <sup>10</sup>P. G. Baines, *Topographic effects in stratified flows* (Cambridge University Press, 1995).
- <sup>11</sup>R. R. Long, “On the Boussinesq approximation and its role in the theory of internal waves,” *Tellus* **17**, 46–52 (1965).
- <sup>12</sup>L. V. Ovsyannikov, “Two-layer “shallow water” model,” *J. Appl. Mech. Tech. Phys.* **20**, 127–135 (1979).
- <sup>13</sup>L. Chumakova, F. E. Menzaque, P. A. Milewski, R. R. Rosales, E. G. Tabak, and C. V. Turner, “Stability properties and nonlinear mappings of two and three-layer stratified flows,” *Stud. Appl. Math.* **122**, 123–137 (2009).
- <sup>14</sup>J. G. Esler and J. D. Pearce, “Dispersive dam-break and lock-exchange flows in a two-layer fluid,” *J. Fluid Mech.* **667**, 555–585 (2011).
- <sup>15</sup>T. B. Benjamin, “Gravity currents and related phenomena,” *J. Fluid Mech.* **31**, 209–248 (1968).
- <sup>16</sup>H. E. Huppert and J. E. Simpson, “The slumping of gravity currents,” *J. Fluid Mech.* **99**, 785–799 (1980).
- <sup>17</sup>J. W. Rottman and J. E. Simpson, “Gravity currents produced by instantaneous releases of a heavy fluid in a rectangular channel,” *J. Fluid Mech.* **135**, 95–110 (1983).
- <sup>18</sup>J. J. Keller and Y.-P. Chyou, “On the hydraulic lock-exchange problem,” *ZAMP* **42**, 874–910 (1991).
- <sup>19</sup>R. J. Lowe, J. W. Rottman, and P. F. Linden, “The non-Boussinesq lock-exchange problem. part 1. theory and experiments,” *J. Fluid Mech.* **537**, 101–124 (2005).

- <sup>20</sup>Z. Borden and E. Meiburg, “Circulation based models for boussinesq gravity currents,” *Phys. Fluids* **25**, 101301 (2013).
- <sup>21</sup>G. B. Whitham, *Linear and Nonlinear Waves* (Wiley, 1974).
- <sup>22</sup>A. J. Hogg, “Lock-release gravity currents and dam-break flows,” *J. Fluid Mech.* **569**, 61–87 (2006).
- <sup>23</sup>M. Ungarish, *An introduction to gravity currents and intrusions* (CRC Press, 2009).
- <sup>24</sup>P. A. Milewski and E. G. Tabak, “Conservation law modelling of entrainment in layered hydrostatic flows,” *J. Fluid Mech.* **772**, 272–294 (2015).
- <sup>25</sup>M. A. Khodkar, M. M. Nasr-Azadani, and E. Meiburg, “Partial-depth lock-release flows,” *Phys. Rev. Fluids* **2**, 064802 (2017).
- <sup>26</sup>J. Pedlosky, *Geophysical fluid dynamics* (Springer, 1979).
- <sup>27</sup>J. Priede, “Self-contained two-layer shallow water theory of strong internal bores,” arXiv:1806.06041 (2020).
- <sup>28</sup>J. B. Klemp, R. Rotunno, and W. C. Skamarock, “On the propagation of internal bores,” *J. Fluid Mech.* **331**, 81–106 (1997).
- <sup>29</sup>I. R. F. Wood and J. E. Simpson, “Jumps in layered miscible fluids,” *J. Fluid Mech.* **140**, 329–342 (1984).
- <sup>30</sup>R. R. Long, “Long waves in a two-fluid system,” *J. Meteor.* **13**, 70–74 (1956).
- <sup>31</sup>A. G. Cavanie, “Sur la genese et la propagation d’ondes internes dans un milieu a deux couches,” *Cahiers Océanographiques* **XXI**, 831–843 (1969).
- <sup>32</sup>H. Sandstrom and C. Quon, “On time-dependent, two-layer flow over topography. i. hydrostatic approximation,” *Fluid Dyn. Res.* **11**, 119 (1993).
- <sup>33</sup>P. Milewski, E. Tabak, C. Turner, R. Rosales, and F. Menzaque, “Nonlinear stability of two-layer flows,” *Comm. Math. Sci.* **2**, 427–442 (2004).
- <sup>34</sup>C.-S. Yih and C. R. Guha, “Hydraulic jump in a fluid system of two layers,” *Tellus* **7**, 358–366 (1955).
- <sup>35</sup>P. G. Baines, “Internal hydraulic jumps in two-layer systems,” *J. Fluid Mech.* **787**, 1–15 (2016).
- <sup>36</sup>C. Härtel, E. Meiburg, and F. Necker, “Analysis and direct numerical simulation of the flow at a gravity-current head. part 1. flow topology and front speed for slip and no-slip boundaries,” *J. Fluid Mech.* **418**, 189–212 (2000).

- <sup>37</sup>R. Liska and B. Wendroff, “Composite schemes for conservation laws,” *SIAM J. Numer. Anal.* **35**, 2250–2271 (1998).
- <sup>38</sup>A. Lerat and R. Peyret, “Noncentered schemes and shock propagation problems,” *Computers & Fluids* **2**, 35–52 (1974).
- <sup>39</sup>Z. Borden and E. Meiburg, “Circulation-based models for Boussinesq internal bores,” *J. Fluid Mech.* **726**, R1 (2013).